

Reversible plasticity in amorphous materials

Micah Lundberg¹, Kapilanjani Krishan¹, Ning Xu^{2,3}, Corey S. O'Hern^{4,5} and Michael Dennin¹

¹*Department of Physics and Astronomy, University of California at Irvine, Irvine, CA 92697-4575*

²*Department of Physics and Astronomy, University of Pennsylvania, Philadelphia, PA 19104-6396*

³*James Franck Institute, The University of Chicago, Chicago, IL 60637*

⁴*Department of Mechanical Engineering, Yale University, New Haven, CT 06520-8286*

⁵*Department of Physics, Yale University, New Haven, CT 06520-8120*

(Dated: February 1, 2008)

A fundamental assumption in our understanding of material rheology is that when microscopic deformations are reversible, the material responds elastically to external loads. Plasticity, i.e. dissipative and irreversible macroscopic changes in a material, is assumed to be the consequence of irreversible microscopic events. Here we show direct evidence for reversible plastic events at the microscopic scale in both experiments and simulations of two-dimensional foam. In the simulations, we demonstrate a link between reversible plastic rearrangement events and pathways in the potential energy landscape of the system. These findings represent a fundamental change in our understanding of materials—microscopic reversibility does not necessarily imply elasticity.

PACS numbers: 05.20.Gg, 05.70.Ln, 83.80.Iz

One of the fundamental questions in materials science concerns the microscopic origin of plastic behavior. Why do materials display plastic rather than elastic and reversible response and can we predict for what loads this will occur? An improved understanding of plastic deformation is especially important in a wide range of amorphous materials, such as metallic[1, 2] and polymeric glasses[3], viscoplastic solids[4], foams[5], granular materials[6], colloids[7, 8], emulsions[9], and even intracellular networks[10]. In crystalline materials, plastic behavior is understood in terms of defect nucleation and dynamics[11, 12]. However, for amorphous materials, a description in terms of topological defects is not possible due to inherent structural disorder. Therefore, identifying and characterizing local plastic events in amorphous materials is essential for a complete understanding of their structural and mechanical properties. The conventional wisdom is that plastic rearrangement events cause irreversible structural changes in these materials on the microscale.

The macroscopic response of amorphous solids and complex fluids, such as foams, colloids, and granular matter, to applied stress and strain is very similar: elastic at small strains and plastic at larger strains. In the elastic regime, stress is proportional to applied strain, and deformations are reversible. Above the yield stress or strain, plastic flow or anelastic deformation occurs. Given these similarities on the macroscopic scale, many models of plasticity have emphasized the importance of microscopic “plastic zones” within amorphous materials[2, 13, 14, 15, 16, 17, 18] in which neighbor switching and other rearrangements events of “particles” occur. (The particles represent molecules in the case of solids, or bubbles or grains in the case of complex fluids.) An important open question concerning plasticity is whether or not plastic zones are intrinsically irreversible or, instead, is their surrounding environment

ultimately responsible for determining whether or not rearrangement events are reversible?

We perform both experiments and simulations of two-dimensional amorphous foams undergoing oscillatory shear strain to investigate this fundamental question. In both cases, we find a significant fraction of dissipative, plastic rearrangement events that are *reversible*, even for strains significantly above the yield strain. In the simulations, measurements of the local potential energy allows us to assess the impact of the bubble’s neighborhood on the reversibility of the plastic events. This links reversible plastic rearrangement events to pathways in the potential energy landscape of the system during deformation. We argue that even during plastic flow certain microscopic rearrangement events are intrinsically reversible and changes in the environment surrounding plastic zones determine whether the zones are reversible or not.

We chose bubble rafts[4, 19, 20, 21] that consist of gas bubbles floating on a water surface for our experimental system. For the simulations, we employed the well-characterized bubble model for two-dimensional (2D) foams developed by Durian[22]. The bubble model assumes massless circular bubbles that interact through a repulsive linear spring force and viscous dissipation. Experimental evidence supports the applicability of the bubble model to explain the flow behavior of bubble rafts, as well as three-dimensional foam[21, 23, 24]. Even though other rearrangement events occur in bubble rafts and the bubble model, plastic rearrangement events known as T1 events play a central role in the mechanical response of foam[20, 21, 25, 26, 27, 28, 29, 30, 31].

T1 events correspond to a neighbor switching event in which two neighboring bubbles lose contact, and two next-nearest neighbors become neighbors[5]. This corresponds to a transition between two distinct states of the system. For example, referring to Fig. 1, State A is when bubbles 1 and 2 are neighbors, and State B is when

bubbles 3 and 4 are neighbors. For both the experiment and the simulations, during one cycle the applied shear strain varies from 0 to A/L_y (at phase $\psi = \pi$) and back to a strain of 0 (at $\psi = 2\pi$), where A is the amplitude of the shear displacement and L_y is the system size in the shear-gradient direction. If four bubbles experience a T1 event that switched the bubbles from state A to B during the first half-cycle of the drive, a reversible T1 event occurs if the same foursome of bubbles returns to state A in the second half-cycle of the drive. Otherwise, the T1 event is irreversible.

For the experiments, the system contained approximately 800 bubbles in a planar shear cell with $L_y = 9$ cm. Half of the bubbles were 2 mm in diameter and the other half were 3.5 mm. We report on results using driving amplitudes A of 10 and 12 times the diameter of the small bubbles and driving frequency 0.2 s^{-1} . The resulting rms strain and strain rate were approximately 0.2 and 0.04 s^{-1} , respectively. This should be compared with the yield strain of 0.01 for bubble rafts and the transition to quasi-static behavior on the order of 0.07 s^{-1} [32]. At the yield strain, T1 events give rise to permanent plastic deformation[33]. Details of the experimental setup for bubble rafts can be found in Ref. [34].

In the bubble model simulations, bidisperse systems composed of $N/2$ large and $N/2$ small circular bubbles with diameter ratio $r = 1.75$ were used to match experiments. We studied square simulation cells with system sizes in the range $N = 16$ to 1024 and packing fraction $\phi = 0.95$, so that the bubbles were always compressed during shear. The bubble model treats foams as massless deformable disks with an equation of motion that balances a linear repulsive spring force to model elastic repulsion with viscous dissipation proportional to local velocity differences[22]. The oscillatory shear strain is applied quasistatically to the system by shifting the x -positions of the bubbles, implementing shear-periodic Lees-Edwards boundary conditions[35] and minimizing the total potential energy. To study the role of the energy landscape, two definitions of the local potential energy based on the overlaps between bubbles were used, E and E' . E is computed only considering overlaps among the four bubbles defining the T1 event, while E' also includes overlaps with the first nearest neighbors of the T1 bubbles. Finally, we measured $\Delta E'$, defined by subtracting the potential energy E' of the four bubbles participating in the reversible T1 event from the original oscillatory shear strain simulations with E' from simulations in which the four T1 bubbles are forced to exactly retrace their positions as they transition from state B back to state A, but all other particles are allowed to move without constraints.

To fully understand the behavior of the system, it is best to directly compare the reversible and irreversible rearrangement events from both experiments and simulation. Panels (a) and (b) of Fig. 1 (experiment) and

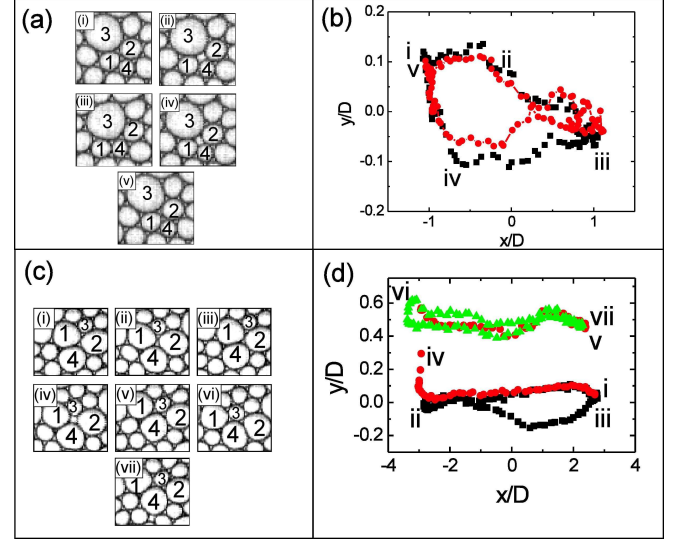


FIG. 1: (color online) Experimental results for a reversible [(a) and (b)] and an irreversible T1 event [(c) and (d)]. The images in (a) and (c) are $10.5 \text{ mm} \times 10.5 \text{ mm}$ with bubbles involved in the T1 events labeled by numbers. The roman label for each image in (a) and (c) corresponds to the same label on the trajectory in (b) and (d). (a) The images highlight the following stages of the reversible T1 event: initial state (i), middle of the T1 event (ii), second state (iii), middle of the T1 event under reversal of shear (iv), and the return to the initial state (v)[36]. (b) Plot of the trajectory of bubble 1 in the images in (a). Two consecutive cycles are shown (the first in black squares and the second in red circles). (c) The images highlight the following stages of the irreversible T1 event: initial state (i - iii), middle of the T1 event (iv), and the second state (v - vii). (d) Plot of the trajectory of bubble 4 in the images in (c). Three consecutive cycles are shown (the first in black, the second in red, the third in green).

Fig. 2 (simulation) highlight typical reversible T1 events. Panels (c) and (d) of Fig. 1 (experiment) and Fig. 2 (simulation) highlight irreversible events. The plots focus on the four bubbles (labeled 1 - 4) that experience a T1 event. Snapshots are used to illustrate bubble motions during a typical T1 event (panels (a) and (c)). For the experiments, panel (b) and (d) highlight the trajectory of a single bubble in real space. For the simulations, panels (b) and (d) display the potential energy E as a function of the phase of the driving. The simulation results are for $N = 16$, but similar results were obtained with much larger systems with $N = 1024$.

The defining feature of reversible T1 events is that the initial and final states of the bubbles in the T1 event are equivalent, despite the occurrence of dissipation. The dissipation is evident in the anharmonic behavior of the local potential energy signal. This is in contrast to the perfectly elastic behavior for small shear strains in the absence of T1 events shown in the inset to Fig. 2b. The existence of the dissipation leads to a number of asymmetries in the dynamics of the system, despite the overall periodic nature of the response. The spatial trajectory

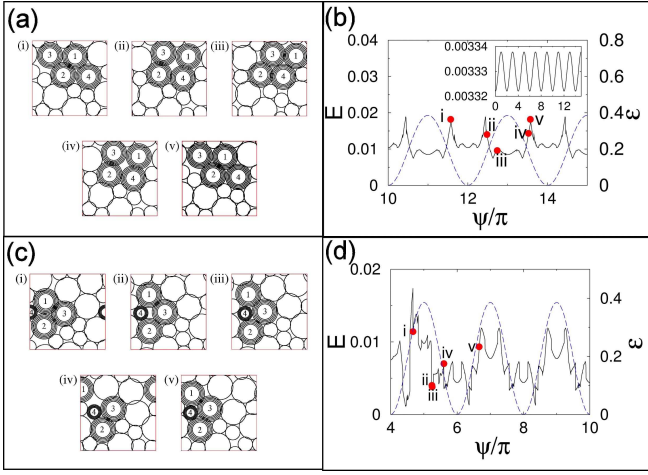


FIG. 2: Results taken from a 16-particle simulation of the bubble model in two dimensions undergoing oscillatory shear strain with an amplitude of 2 small bubble diameters for a reversible [(a) and (b)] and an irreversible event [(c) and (d)]. Bubbles involved in the T1 events are labeled by numbers. Roman labels in the images correspond to the same labels in the plots. (a) Images (i)-(iii) show the occurrence of a reversible T1 event and (iv) and (v) show the reversal of the T1 event. (See the supplementary information for a movie of this event.) (b) The local potential energy E (solid black line) is plotted versus the driving phase (left axis). For comparison, the periodic strain is plotted with a long dashed blue line (right axis). The elapsed phase for the T1 event is significantly different than that for the reversed T1 event, and the shape of the local potential energy is not the same for the T1 event and its reverse. The inset shows an elastic response in E vs ψ/π for small amplitude oscillations $A = 10^{-2}$ times the small bubble diameter, where the response matches the driving. (c) Images (i)-(iii) show the occurrence of an irreversible T1 event, as shown by the absence of the reverse T1 event in images (iv) and (v)[36]. (d) The local potential energy E (solid black line) is plotted versus the driving phase (left axis). The periodic strain is plotted with a long dashed blue line (right axis). Note that E for locations (i) and (v) separated by a phase interval of 2π are not the same.

is a closed loop with a finite area (see Fig. 1b). This causes the symmetric rearrangements of the four bubbles during the two T1 events (images (ii) and (iv) in Fig. 1a) to occur at different locations during the corresponding half-cycle. Likewise, Fig. 2b illustrates that E is very different for the two half cycles corresponding to labels (i)-(iii) and (iv)-(v). Finally, the durations of the T1 event and its reverse (state A to B vs. state B to A) are not the same.

During irreversible T1 events, the defining feature is that a foursome of bubbles undergoes a T1 event in the first half cycle of the driving but the reverse T1 event does not occur during the second half cycle. The experimental example in Fig. 1c is a case where a single T1 event from state A to B occurred during seven cycles of the driving (three of which are highlighted in Fig. 1c). The impact of the T1 event on the trajectories in Fig. 1d is dramatic. The trajectory of bubble four is shown for

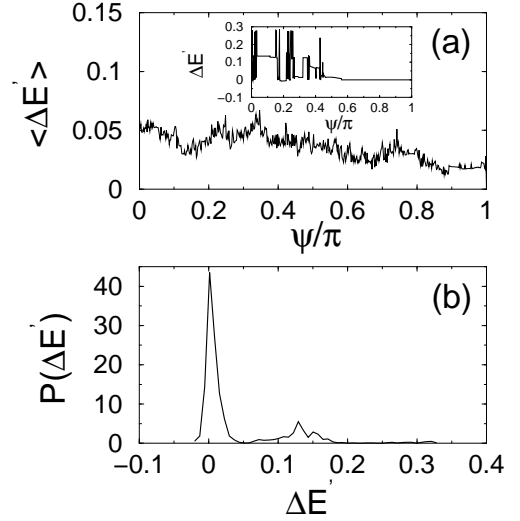


FIG. 3: (a) The local potential energy difference $\langle \Delta E' \rangle$ averaged over 100 reversible T1 events plotted vs. the driving phase under the same conditions in Fig. 2. $\langle \Delta E' \rangle > 0$ confirms that *exact* trajectory reversal is not energetically favorable. The inset shows $\Delta E'$ for a single reversible T1 event. (b) The probability of finding a particular $\Delta E'$. There is a large peak at $\Delta E' = 0$, two slight peaks near 0.15 and 0.30, and no significant weight in the distribution for $\Delta E' < 0$.

three cycles: just before the T1 event (black), during the T1 event (red), and just after the T1 event (green). In the absence of a T1 event, the local trajectory essentially repeats itself during each half-cycle as the bubbles move along similar paths. The occurrence of the T1 event represents a dramatic break in this motion.

The behavior of irreversible T1 events in simulations is similar to that found in experiments. Figure 2c illustrates a T1 event that occurs during frames (i)-(iii) in the first half cycle, but the T1 event is not reversed during the second half cycle in frames (iii)-(v). The plot of E in Fig. 2(d) illustrates that configurations (i) and (v), which are separated by 2π in phase, do not have the same local potential energy. Note that beyond $\psi/\pi \sim 5.5$, the local potential energy signal is periodic, which indicates that other T1 events or possibly more complex rearrangement events that occur in the system are reversible.

What is the connection between reversible T1 events and the path that the system follows through the potential energy landscape? Answering this question provides initial insights into why some T1 events are reversible and others are irreversible and how the system returns to the same potential energy minimum even though it follows a different path in the energy landscape during the T1 event and its reverse. The calculation of $\Delta E'$ obtained by comparing the local potential energy E' (including interactions of T1 bubbles with first nearest neighbors) of the four bubbles in the original oscillatory shear strain simulations with E' from the constrained simulations directly addresses this question.

The results from these studies are shown in Fig. 3. First, in Fig. 3(a) we find that the local potential energy

difference averaged over many T1 events from independent runs $\langle \Delta E' \rangle > 0$. $\Delta E'$ for a single T1 event shown in the inset to Fig. 5(a) has large positive spikes but also significant phase intervals where $\Delta E' = 0$. In Fig. 3(b), we show that the distribution $P(\Delta E')$ of energy differences has a strong peak at zero, but non-negligible peaks at $\Delta E' \approx 0.15$ and 0.3 and no significant weight for $\Delta E' < 0$. Each of these findings indicates that the path during the second half cycle that does not exactly retrace the path in configuration space of the first half cycle is energetically favorable. Furthermore, for the case of reversible T1 events, it is likely that there are a number of local low energy pathways that lead from state B back to state A. For the case of irreversible T1 events, it is likely that there are many local energy pathways away from state B, but the ones that are energetically favorable do not lead back to state A. Since our system is athermal, these differences in the energy pathways are due to changes in the environment (surrounding bubbles) that occur during the applied shear strain. Thus, we argue that the influence of the environment gives rise to the irreversibility of T1 events in foams. In equilibrium systems, thermal fluctuations will also play a significant role in determining reversibility.

Our experiments and simulations of model foams undergoing oscillatory shear strain identify reversible T1 events, which are two state systems. This observation is the first direct experimental confirmation of a general two-state model of plasticity: shear transformation zones (STZ). The concept of a STZ as a reversible, two-state transition within a material was first proposed by Falk and Langer[14]. The STZ picture is successful in explaining a range of macroscopic behavior of materials based on dynamics of the microstructure. STZ's represent a natural extension of ideas based on activated transitions and free volume[1, 37, 38] and it has motivated a number of other models of plasticity[18, 39, 40]. Therefore, our results establish the applicability of two-state STZ models to athermal particulate systems, and the need to include intrinsically reversible plastic events in models of plasticity. Our studies of the local potential energy landscape go beyond the two-state model and establish the importance of the accessible pathways in the energy landscape that ultimately determine the reversibility of the plastic events. Thus, we have learned that plasticity does not imply microscopic irreversibility and that microscopic reversibility does not imply elasticity.

Financial support from the Department of Energy grant numbers DE-FG02-03ED46071 (MD), DE-FG02-05ER46199 (NX), and DE-FG02-03ER46088 (NX), NSF grant numbers DMR-0448838 (CSO, GL) and CBET-0625149 (CSO), and the Institute for Complex Adaptive Matter (KK) is gratefully acknowledged. We also thank M. Falk for insightful conversations.

-
- [1] A. S. Argon, *Acta Metallurgica* **27**, 47 (1979).
 - [2] M. L. Falk, J. S. Langer, and L. Pechenik, *Physical Review E* **70**, 011507 (2004).
 - [3] M. D. Ediger, *Annual Review Of Physical Chemistry* **51**, 99 (2000).
 - [4] L. Bragg, *Journal of Scientific Instruments* **19**, 148 (1942).
 - [5] D. Weaire and S. Hutzler, *The Physics of Foams* (Clarendon Press, Oxford, 1999).
 - [6] C. H. Liu and S. R. Nagel, *Phys. Rev. B* **48**, 15646 (1993).
 - [7] E. R. Weeks, J. C. Crocker, A. C. Levitt, A. Schofield, and D. A. Weitz, *Science* **287**, 627 (2000).
 - [8] E. R. Weeks and D. A. Weitz, *Physical Review Letters* **89**, 095704 (2002).
 - [9] T. G. Mason, J. Bibette, and D. A. Weitz, *Journal of Colloid and Interface Science* **179**, 439 (1996).
 - [10] D. A. Head, A. J. Levine, and F. C. MacKintosh, *Physical Review E* **68**, 061907 (2003).
 - [11] J. R. Rice and R. Thomson, *Philosophical Magazine* **29**, 73 (1974).
 - [12] J. R. Rice, *Journal Of The Mechanics And Physics Of Solids* **40**, 239 (1992).
 - [13] J. C. Baret, D. Vandembroucq, and S. Roux, *Physical Review Letters* **89**, 195506 (2002).
 - [14] M. L. Falk and J. S. Langer, *Physical Review E* **57**, 7192 (1998).
 - [15] M. Heggen, F. Spaepen, and M. Feuerbacher, *Journal Of Applied Physics* **97**, 033506 (2005).
 - [16] J. S. Langer, *Physical Review E* **73**, 041504 (2006).
 - [17] A. Onuki, *Physical Review E* **68**, 061502 (2003).
 - [18] G. Picard, A. Ajdari, L. Bocquet, and F. Lequeux, *Physical Review E* **66**, 051501 (2002).
 - [19] A. S. Argon and H. Y. Kuo, *Materials Science And Engineering* **39**, 101 (1979).
 - [20] A. Abdel Kader and J. C. Earnshaw, *Physical Review Letters* **82**, 2610 (1999).
 - [21] M. Dennin, *Physical Review E* **70**, 041406 (2004).
 - [22] D. J. Durian, *Phys. Rev. Lett.* **75**, 4780 (1995).
 - [23] J. Lauridsen, M. Twardos, and M. Dennin, *Physical Review Letters* **89**, 098303 (2002).
 - [24] A. D. Gopal and D. J. Durian, *Physical Review Letters* **75**, 2610 (1995).
 - [25] Y. Wang, K. Krishan, and M. Dennin, *Philosophical Magazine Letters* **87**, 125 (2007).
 - [26] M. Dennin and C. M. Knobler, *Physical Review Letters* **78**, 2485 (1997).
 - [27] B. Dollet, M. Durth, and F. Graner, *Physical Review E* **73**, 061404 (2006).
 - [28] D. A. Reinelt and A. M. Kraynik, *J. Rheol. (N. Y.)* **44**, 453 (2000).
 - [29] M. F. Vaz and S. J. Cox, *Philosophical Magazine Letters* **85**, 415 (2005).
 - [30] D. Weaire, F. Bolton, T. Herdtle, and H. Aref, *Phil. Mag. Lett.* **66**, 293 (1992).
 - [31] S. Vincent-Bonnieu, R. H. Hohler, and S. Cohen-Addad, *Europhysics Letters* **74**, 533 (2006).
 - [32] E. Pratt and M. Dennin, *Physical Review E* **67**, 051402 (2003).
 - [33] S. Hutzler, Ph.D. thesis, Trinity College, Dublin (1997).
 - [34] M. Lundberg, K. Krishan, N. Xu, C. S. O'Hern, and M. Dennin, in preparation (2007).

- [35] M. P. Allen and D. J. Tildesley, *Computer Simulation of Liquids* (Oxford University Press, Oxford, 1987).
- [36] See EPAPS Document No. [] for movies of the reversible (ExperimentReversible.mov, SimulationReversible.mov) and irreversible (ExperimentIrreversible.mov, SimulationIrreversible.mov) events from both the experiments and simulation. For more information on EPAPS, see <http://www.aip.org/pubservs/epaps.html>.
- [37] V. A. Khonik and A. T. Kosilov, *Journal Of Non-Crystalline Solids* **170**, 270 (1994).
- [38] F. Spaepen, *Acta Metallurgica* **25**, 407 (1977).
- [39] L. Berthier, *Journal Of Physics-Condensed Matter* **15**, S933 (2003).
- [40] G. Picard, A. Ajdari, F. Lequeux, and L. Bocquet, *European Physical Journal E* **15**, 371 (2004).